

Development of methods for paired single-cell multimodal integration

Geert-Jan Huizing

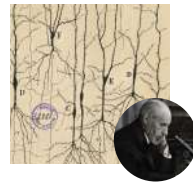
Thesis defense, September 27th, 2024

Ecole doctorale 515. Thesis directors: Laura Cantini & Gabriel Peyré

Uncovering cellular heterogeneity



$\sim 10^{13}$ cells in the human body,
with vastly different functions.



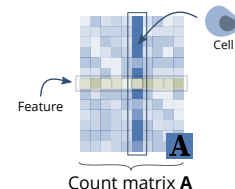
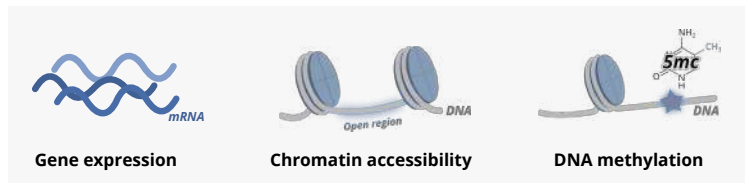
Early efforts to cartography
cell identity relied on microscopy¹.



Recent initiatives measure the
molecular profile of the cell².

¹Ramón y Cajal, 1899; ²Regev et al., *eLife*, 2017

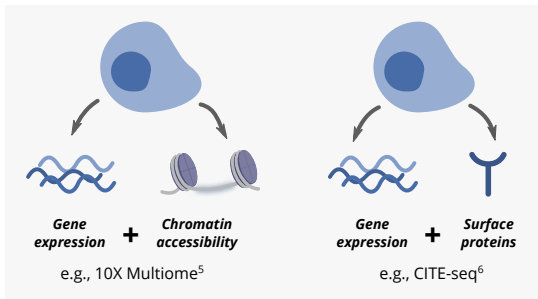
Single-cell omics sequencing



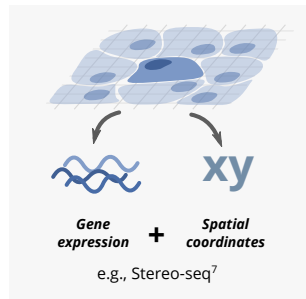
Single-cell sequencing technologies^{3,4} deliver quantitative *omics* information as a count matrix.

³Nawy, *Nature methods*, 2014; ⁴Preissl et al., *Nature Reviews Genetics*, 2023

Multimodal omics sequencing



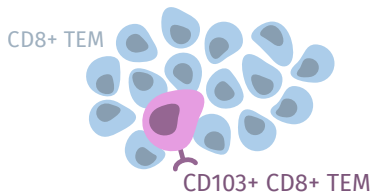
Single-cell multi-omics measure the cell at several molecular layers.



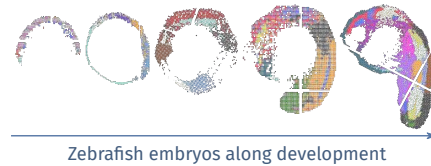
Spatial omics measure the cell without dissociating the tissue.

⁵10X Genomics; ⁶Stoeckius et al., *Nature methods*, 2017; ⁷Chen et al., *Cell*, 2022

Applications of multimodal omics



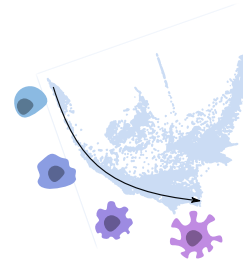
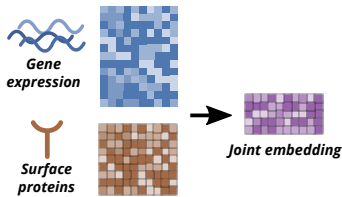
The joint profiling of **gene expression and surface proteins** enabled to identify a new subpopulation of CD8 TEM cells⁸.



Spatial transcriptomics profiled across time have allowed to study development at unprecedented resolution⁹.

⁸Hao et al., *Cell*, 2021; ⁹Liu et al., *Developmental Cell*, 2022

Paired single-cell multimodal integration



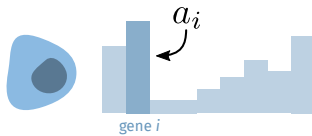
Joint dimensionality reduction can discover patterns across modalities and identify cell subpopulations^{10,11}.

Trajectory inference, which can discover trends along a dynamic process such as development, aging or regeneration^{12,13}.

¹⁰ Argelaguet et al., *Genome biology*, 2020; ¹¹ Lotfollahi et al., *bioRxiv*, 2022; ¹² Li et al., *Nature biotechnology*, 2023; ¹³ Klein et al., *bioRxiv*, 2023

Formalizing cells and populations

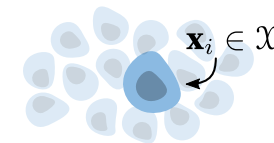
Unifying notation across this presentation: $\mu = \sum_i a_i \delta_{\mathbf{x}_i}$ with $\mathbf{a} \in \Sigma_n$ and $\mathbf{x}_i \in \mathcal{X}$



$$\mu = \sum_i a_i \delta_{\mathbf{x}_i} \text{ with } \mathbf{a} \in \Sigma_n \text{ and } \mathbf{x}_i \in \mathcal{X}$$

cell **gene**

We formalize the cell as a histogram over the space of molecular features,

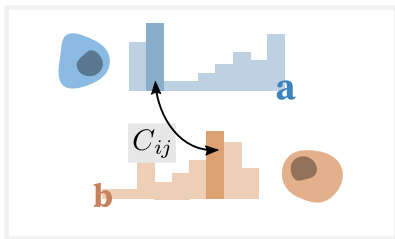


$$\mu = \sum_i a_i \delta_{\mathbf{x}_i} \text{ with } \mathbf{a} \in \Sigma_n \text{ and } \mathbf{x}_i \in \mathcal{X}$$

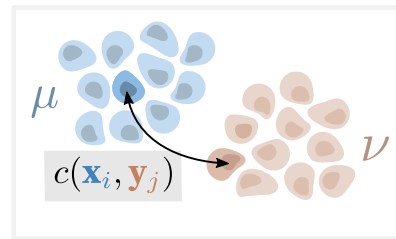
cell

and populations of cells as a point cloud over some Euclidean space \mathcal{X} .

Optimal Transport compares distributions



Eulerian setting: $W_C(\mathbf{a}, \mathbf{b})$

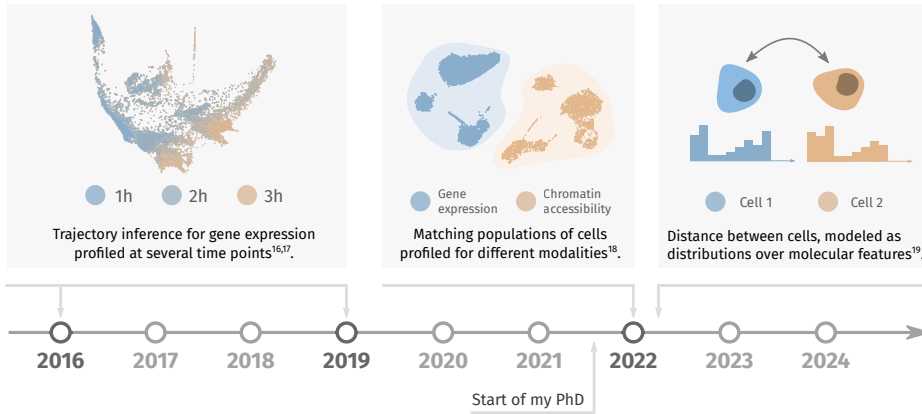


Lagrangian setting: $\mathcal{W}_c(\mu, \nu)$

Optimal Transport^{14,15} is a mathematical framework to compare probability distributions.

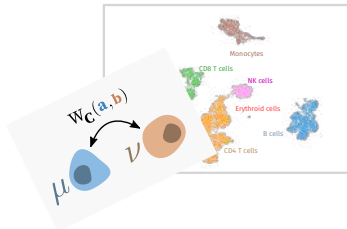
¹⁴Monge, *Mem. Math. Phys. Acad. Royale Sci.*, 1781; ¹⁵Kantorovich, *Doklady Akademii Nauk*, 1942

Applications of Optimal Transport in single-cell data

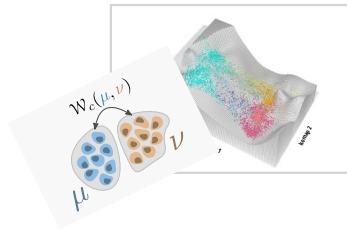


¹⁶ Hashimoto et al., ICML, 2016; ¹⁷ Schiebinger et al., Cell, 2019; ¹⁸ Demetci et al., Journal of Comp. Biology, 2022; ¹⁹ Huizing et al., Bioinformatics, 2022

Aims of this thesis

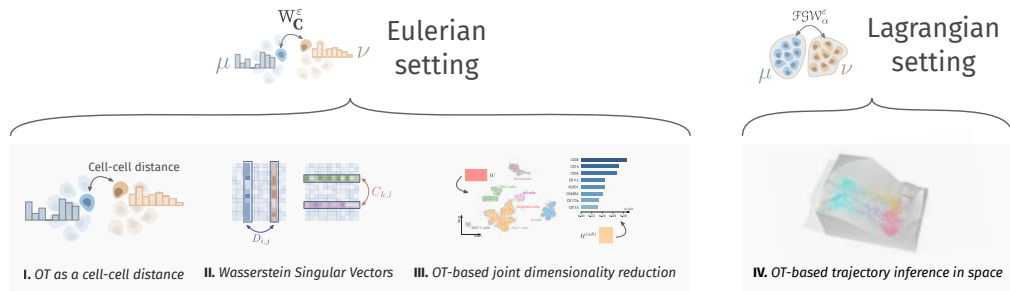


Leverage a cost between features
for **joint dimensionality reduction**
of single-cell **multiomics**.



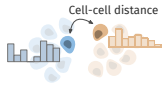
Leverage spatial information in
trajectory inference with spatial
transcriptomics through time.

Contributions of this thesis

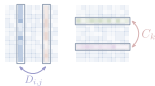


Optimal Transport improves cell-cell similarity inference in single-cell omics data

Work published as: G.-J. Huizing, G. Peyré, L. Cantini, *Bioinformatics*, 2022



I. OT as a cell-cell distance



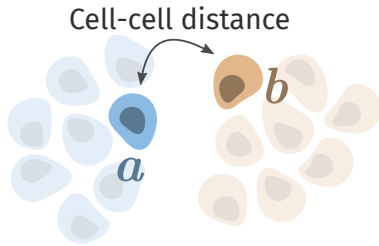
II. Wasserstein Singular Vectors



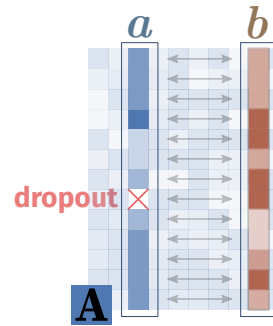
III. OT-based joint dimensionality reduction



Distances between cells

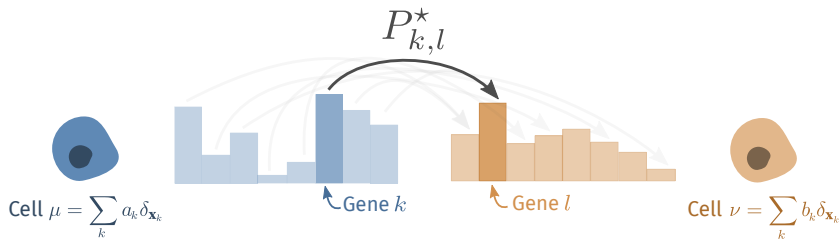


Distances between cells are crucial for downstream tasks (e.g., clustering).



Bin-bin distances like the Euclidean distance compare genes one by one.

Optimal Transport distances between cells

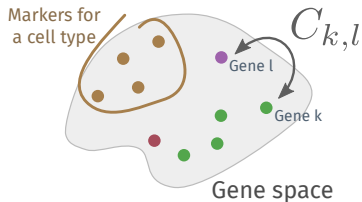


$$W_C(\mathbf{a}, \mathbf{b}) \stackrel{\text{def.}}{=} \min_{\mathbf{P} \in \mathcal{U}(\mathbf{a}, \mathbf{b})} \sum_{k,l} C_{k,l} P_{k,l} \quad \text{with } \mathcal{U}(\mathbf{a}, \mathbf{b}) \stackrel{\text{def.}}{=} \{\mathbf{P} \in \mathbb{R}_+^{m \times m}, \mathbf{P}\mathbf{1}_m = \mathbf{a}, \mathbf{P}^\top \mathbf{1}_m = \mathbf{b}\}$$

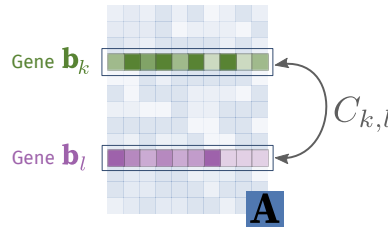
Optimal Transport^{20,21} defines a distance between distributions as the cost of transporting mass from one to the other.

²⁰Monge, *Mem. Math. Phys. Acad. Royale Sci.*, 1781; ²¹Kantorovich, *Doklady Akademii Nauk*, 1942

Ground cost for single-cell omics



Similar features, like markers for the same cell type, should have a low cost.



$$1 - \cos(\mathbf{b}_k, \mathbf{b}_l) = 1 - \frac{\mathbf{b}_k^T \mathbf{b}_l}{\|\mathbf{b}_k\|_2 \|\mathbf{b}_l\|_2}$$

Here, we consider distances between rows of the cost matrix, but alternatives exist^{24,25}.

²⁴Bellazi et al., arXiv, 2021; ²⁵Huizing et al., ICML, 2022

Entropic regularization of Optimal Transport

Entropy-regularized Optimal Transport²² is a fast approximation of the previous problem. It can be computed efficiently using the GPU-enabled Sinkhorn algorithm.

$$W_C^\varepsilon(\mathbf{a}, \mathbf{b}) \stackrel{\text{def.}}{=} \min_{\mathbf{P} \in \mathcal{U}(\mathbf{a}, \mathbf{b})} \sum_{k,l} C_{k,l} P_{k,l} - \varepsilon E(\mathbf{P}),$$

$$\text{where } E : \mathbf{P} \mapsto - \sum_{k,l} P_{k,l} (\log P_{k,l} - 1)$$

The **Sinkhorn divergence**²³ eliminates the bias introduced by the entropic regularization.

$$\overline{W_C^\varepsilon}(\mathbf{a}, \mathbf{b}) \stackrel{\text{def.}}{=} W_C^\varepsilon(\mathbf{a}, \mathbf{b}) - \frac{1}{2} (W_C^\varepsilon(\mathbf{a}, \mathbf{a}) + W_C^\varepsilon(\mathbf{b}, \mathbf{b})).$$

²²Cuturi, NeurIPS, 2013; ²³Genevay et al., AISTATS, 2018

Introduction
oooooooooooo

OT as a cell-cell distance
oooo●●oooo

Wasserstein Singular Vectors
oooooooooo

OT-based joint dimensionality reduction
oooooooooo

OT-based trajectory inference
oooooooooooooooooooo

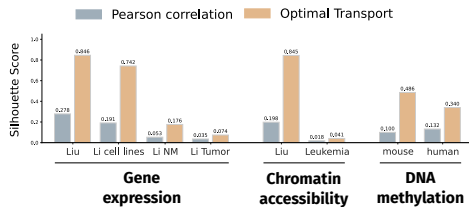
Conclusion
oooooo

OT distances better reflect known heterogeneity

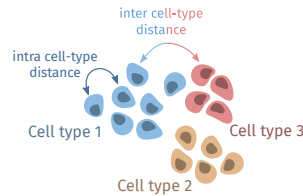
Liu	Li cell lines	Li NM	Li Tumor	Liu	Leukemia	mouse	human
Gene expression				Chromatin accessibility			
DNA methylation							

We consider several datasets across three
omics annotated with cell types.

OT distances better reflect known heterogeneity

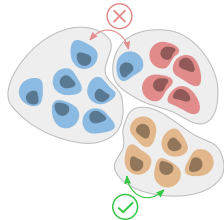


We consider several datasets across three omics annotated with cell types.



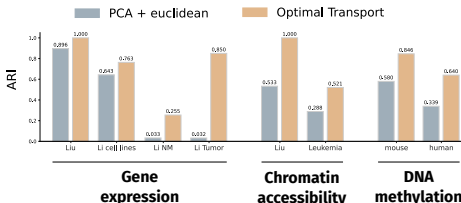
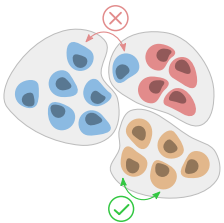
We compare OT to common bin-bin distances using the Silhouette score.

OT-based clustering outperforms the standard approach



We also evaluate clustering performance using the Adjusted Rand Index.

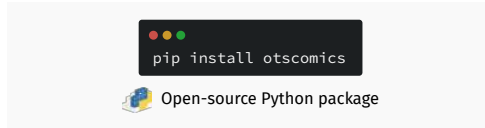
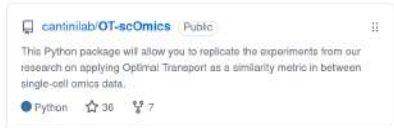
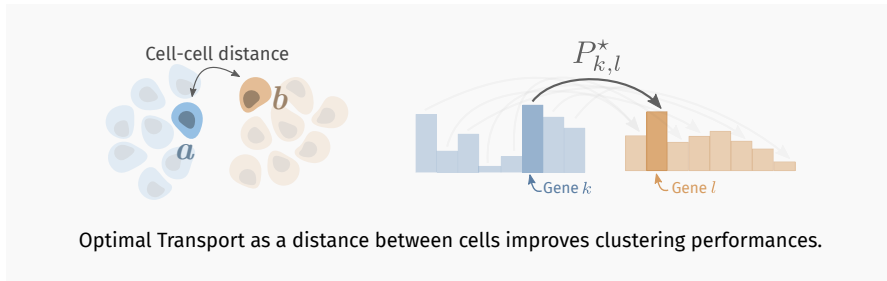
OT-based clustering outperforms the standard approach



We also evaluate clustering performance using the Adjusted Rand Index.

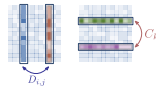
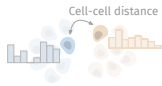
We use Leiden clustering based on OT, and the standard Euclidean distance on PCA.

Conclusion



Unsupervised ground metric learning using Wasserstein Singular Vectors

Work published as: G.-J. Huizing, L. Cantini, G. Peyré, ICML, 2022



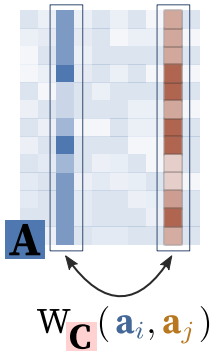
I. OT as a cell-cell distance

II. Wasserstein Singular Vectors

III. OT-based joint dimensionality reduction

IV. OT-based trajectory inference in space

Ground metric learning



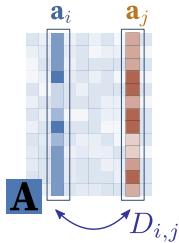
In the previous chapter, we computed cell-cell Optimal Transport distances using a cost **C**.

In a supervised setting, it is possible to learn a ground cost that reflects labels^{26,27}.

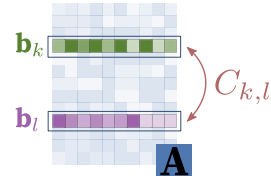
We proposed the first **unsupervised** ground metric learning method.

²⁶Cuturi and Avis, JMLR, 2014; ²⁷Wang and Guibas, ECCV, 2012

Bootstrapping intuition



A central diagram showing the calculation of distances. It consists of two main parts: $D_{i,j} = W_{\mathbf{C}}(\mathbf{a}_i, \mathbf{a}_j)$ and $C_{k,l} = W_{\mathbf{D}}(\mathbf{b}_k, \mathbf{b}_l)$. The first part is labeled "Distance between cells" with a blue arrow pointing to it. The second part is labeled "Distance between features" with a red arrow pointing to it. Curved arrows also connect the two parts to each other.



The transposed problem defines a Wasserstein distance matrix between genes.

Wasserstein Singular Vectors

Let us define a Wasserstein distance map: $\Phi_{\mathbf{A}}(\mathbf{C})_{i,j} \stackrel{\text{def.}}{=} W_{\mathbf{C}}(\mathbf{a}_i, \mathbf{a}_j)$

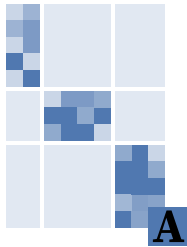
The fixed point condition for the previous bootstrapping algorithm is a **nonlinear singular vectors** problem:

$$\Phi_{\mathbf{A}}(\mathbf{C}) = \gamma \mathbf{D}, \quad \Phi_{\mathbf{B}}(\mathbf{D}) = \lambda \mathbf{C} \quad \text{with } (\lambda, \gamma) \in (\mathbb{R}_+^*)^2 \quad (1)$$

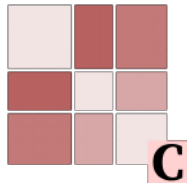
Distance between cells

Distance between features

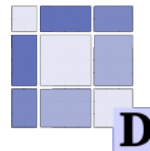

Wasserstein Singular Vectors of a block-diagonal matrix



Consider a block diagonal count matrix.



Pairs **C,D** of block constant and antidiagonal distance matrices are Wasserstein Singular Vectors.



Computing Wasserstein Singular Vectors

We now add a regularization term to the Wasserstein distance map:

$$\Phi_{\mathbf{A}}(\mathbf{C})_{i,j} \stackrel{\text{def.}}{=} W_{\mathbf{C}}(\mathbf{a}_i, \mathbf{a}_j) + \tau \|\mathbf{a}_i - \mathbf{a}_j\|_1$$

Theorem. When $\tau > 0$, there exist positive singular vectors (\mathbf{C}, \mathbf{D}) solving (1).

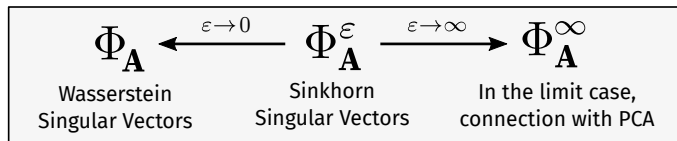
To compute Wasserstein Singular Vectors, we can use the following power iterations:

$$\mathbf{C}_{t+1} \stackrel{\text{def.}}{=} \frac{\Phi_{\mathbf{B}}(\mathbf{D}_t)}{\|\Phi_{\mathbf{B}}(\mathbf{D}_t)\|_\infty}, \quad \mathbf{D}_{t+1} \stackrel{\text{def.}}{=} \frac{\Phi_{\mathbf{A}}(\mathbf{C}_{t+1})}{\|\Phi_{\mathbf{A}}(\mathbf{C}_{t+1})\|_\infty}.$$

In practice, power iterations converge even for $\tau = 0$.

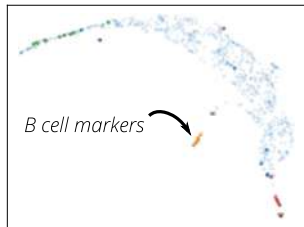
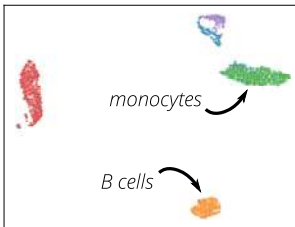
Entropic regularization

Sinkhorn divergence map: $\Phi_{\mathbf{A}}^{\varepsilon}(\mathbf{C})_{i,j} \stackrel{\text{def.}}{=} \overline{W_{\mathbf{C}}^{\varepsilon}}(\mathbf{a}_i, \mathbf{a}_j) + \tau \|\mathbf{a}_i - \mathbf{a}_j\|_1$



In the limit case, $\Phi_{\mathbf{A}}^{\infty} \stackrel{\text{def.}}{=} (-\frac{1}{2} \langle \mathbf{C}(\mathbf{a}_k - \mathbf{a}_l), \mathbf{a}_k - \mathbf{a}_l \rangle)_{k,l}$,
when \mathbf{A} is bistochastic, we can explicit some singular vectors.

Sinkhorn Singular Vectors for single-cell gene expression

UMAP projection of
gene-gene distances $\mathbf{C}_{k,l}$ UMAP projection of
cell-cell distances $\mathbf{D}_{i,j}$

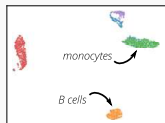
Silhouette score for cells

Method	Silhouette
PCA / ℓ^2	0.238
Kernel PCA / ℓ^2	0.241
scVI embedding / ℓ^2	0.168
Sinkhorn	0.003
Gene Mover Distance	0.066
WSV (ours)	0.348

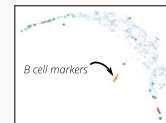
Silhouette score for marker genes

ℓ^2	Gene2Vec / ℓ^2	WSV (ours)
-0.005	0.0186	0.136

Conclusion



$$D_{i,j} = \frac{1}{\gamma} W_{\mathbf{C}}(\mathbf{a}_i, \mathbf{a}_j), \quad C_{k,l} = \frac{1}{\lambda} W_{\mathbf{D}}(\mathbf{b}_k, \mathbf{b}_l)$$



Unsupervised ground metric learning framed as a nonlinear singular vector problem.

CSDUlm/wsingular Public

Python package for the ICML 2022 paper "Unsupervised Ground Metric Learning Using Wasserstein Singular Vectors".

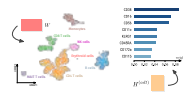
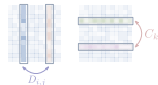
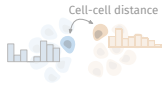
Python ⭐ 9

pip install wsingular

Open-source Python package

Paired single-cell multi-omics data integration with Mowgli

Work published as: G.-J. Huizing, I. M. Deutschmann, G. Peyré, L. Cantini, *Nature Comms*, 2023



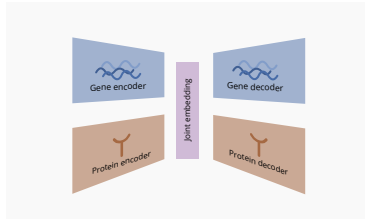
I. OT as a cell-cell distance

II. Wasserstein Singular Vectors

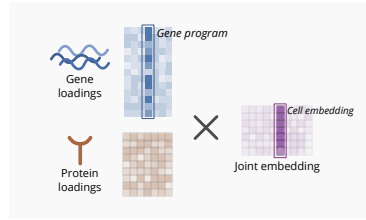
III. OT-based joint dimensionality reduction

IV. OT-based trajectory inference in space

Joint dimensionality reduction methods



Deep learning methods^{28,29} are expressive but lack interpretability.

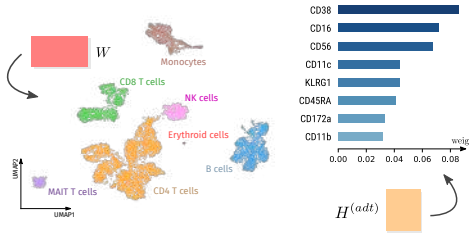


Matrix factorization methods^{30,31} are less expressive but interpretable.

²⁸Gong et al., *Genome biology*, 2021; ²⁹Lotfollahi et al., *bioRxiv*, 2022; ³⁰Argelaguet et al., *Genome biology*, 2020; ³¹Chalise and Fridley, *PloS one*, 2017

Overview of our approach

$$\begin{array}{ccc} A^{(rna)} & & H^{(rna)} \\ & = & \\ A^{(adt)} & = & H^{(adt)} \times W \\ & \cdots & \cdots \end{array}$$



We developed **Mowgli**, a joint Nonnegative Matrix Factorization method with an OT objective.

The joint embedding allows clustering and visualization, and omics-specific loadings enable to interpret results.

Objective function

$$\begin{matrix} A^{(rna)} \\ A^{(adt)} \\ A^{(atac)} \\ \dots \end{matrix} = \begin{matrix} H^{(rna)} \\ H^{(adt)} \\ H^{(atac)} \\ \dots \end{matrix} \times \begin{matrix} W \end{matrix}$$
$$\min_{\mathbf{H}^{(p)}, \mathbf{W}} \sum_p \left(\underbrace{\sum_j \mathbf{W}_{\mathbf{C}^{(p)}}^\varepsilon(\mathbf{H}^{(p)} \mathbf{w}_j, \mathbf{a}_j^{(p)})}_{\text{Reconstruction term}} - \alpha_p \mathbf{E}(\mathbf{H}^{(p)}) - \beta \mathbf{E}(\mathbf{W}) \right)$$

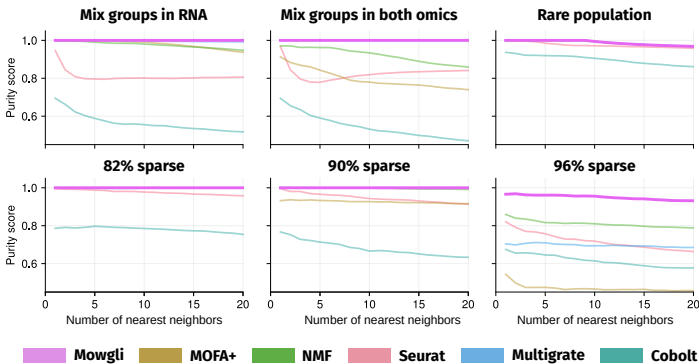
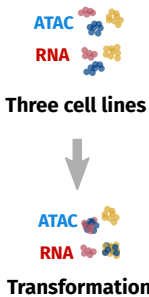
Sum over omics

Reconstruction term Regularization terms

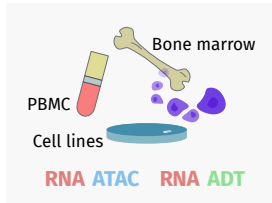
Our objective function extends **Wasserstein NMF**³² to the multimodal setting.

³²Rolet et al., AISTATS, 2016

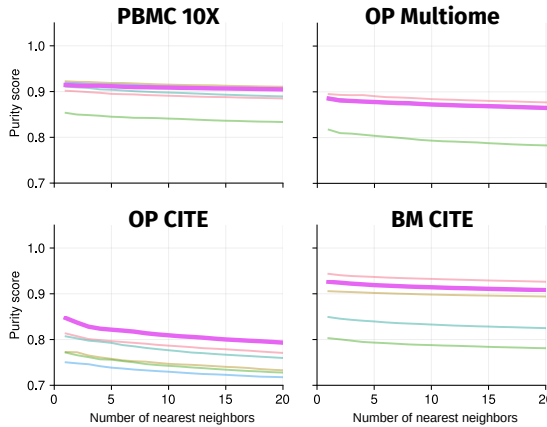
Improved embedding and clustering performance in controlled settings



Competitive embedding and clustering performance in large datasets

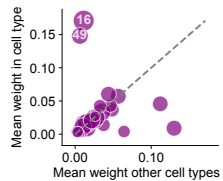


Several conditions and sequencing platforms

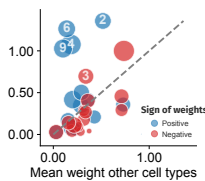


Mowgli MOFA+ NMF Seurat Multigrate Cobolt

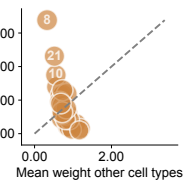
Cell-type specificity of the factors



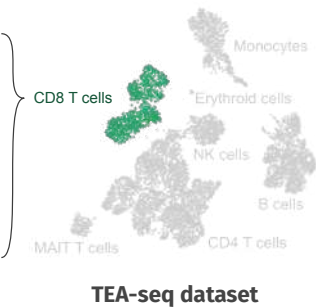
Mowgli



MOFA+

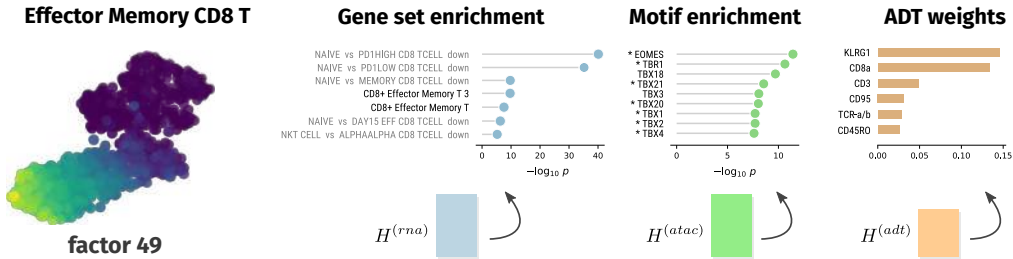


NMF

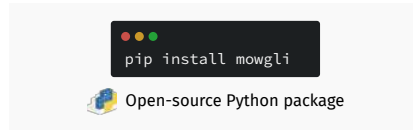
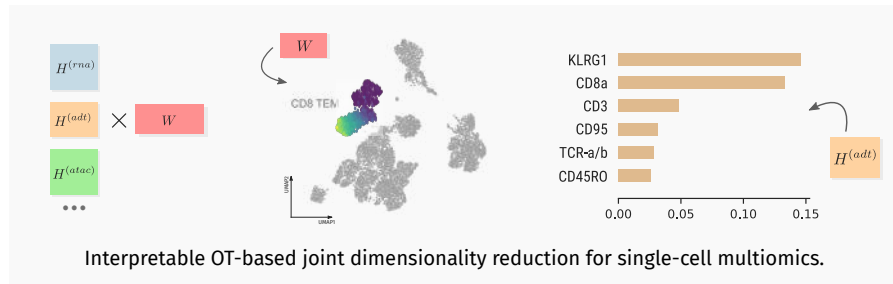


RNA ATAC ADT

Loadings allow to interpret specific factors

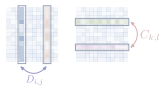
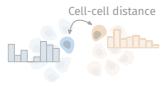


Conclusion



Learning cell fate landscapes from spatial transcriptomics using Fused Gromov-Wasserstein

Preprint: G.-J. Huizing, G. Peyré, L. Cantini, *bioRxiv*, 2024



I. OT as a cell-cell distance

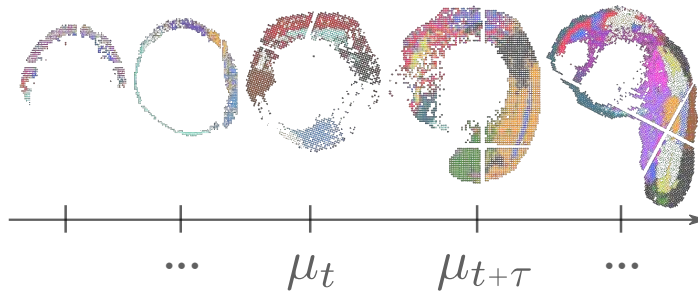
II. Wasserstein Singular Vectors

III. OT-based joint dimensionality reduction

IV. OT-based trajectory inference in space

Lagrangian setting

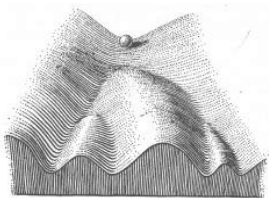
Spatial transcriptomics through time



Recent datasets have profiled spatial transcriptomics at several timepoints^{33,34,35}.

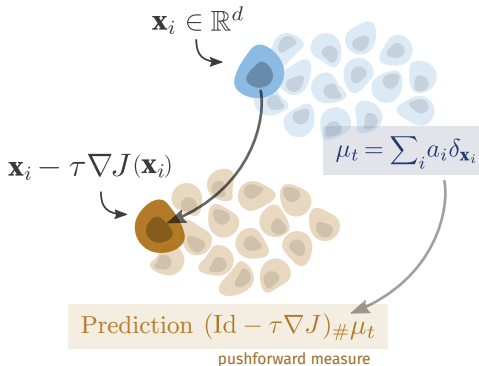
³³Liu et al., *Developmental Cell*, 2022; ³⁴Chen et al., *Cell*, 2022; ³⁵Wei et al., *Science*, 2022

Potential landscapes



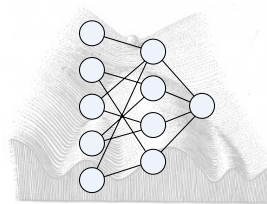
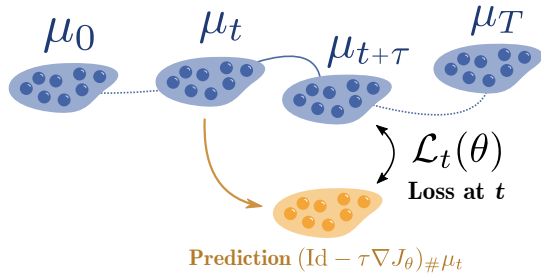
Potential $J : \mathbb{R}^d \rightarrow \mathbb{R}$

Recent trajectory inference methods^{36,37,38}
model cellular differentiation as the
minimization of a **potential energy**.



³⁶Hashimoto et al., ICML, 2016; ³⁷Yeo et al., Nature communications, 2021; ³⁸Bunne et al., AISTATS, 2022

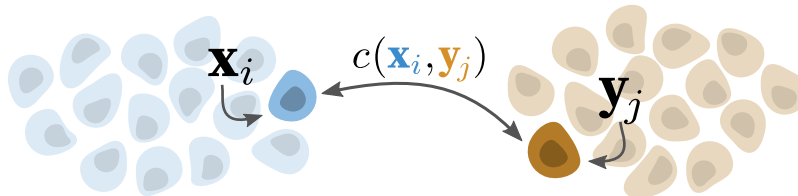
Learning cell fate landscapes using time course data



They learn a potential J_θ by comparing the model's predictions to the true distribution using Optimal Transport^{39,30,41}.

³⁹ Hashimoto et al., ICML, 2016; ⁴⁰ Yeo et al., Nature communications, 2021; ⁴¹ Bunne et al., AISTATS, 2022

Sinkhorn loss

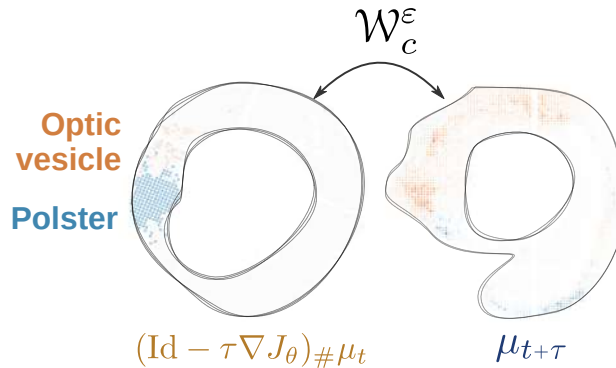


Ground truth $\mu_{t+\tau} = \sum_i a_i \delta_{\mathbf{x}_i}$

Prediction $\nu_{t+\tau} = (\text{Id} - \tau \nabla J)_{\#} \mu_t$

$$\mathcal{W}_c^\varepsilon(\mu_{t+\tau}, \nu_{t+\tau}) \stackrel{\text{def.}}{=} \min_{\mathbf{P} \in \mathcal{U}(\mathbf{a}, \mathbf{b})} \sum_{i,j} c(\mathbf{x}_i, \mathbf{y}_j) P_{i,j} - \varepsilon \mathbf{E}(\mathbf{P})$$

The Sinkhorn loss is not spatially coherent



But the Sinkhorn loss matches regions that are not coherent in space.

Fused Gromov-Wasserstein loss

We propose using Fused Gromov-Wasserstein⁴² to leverage space.

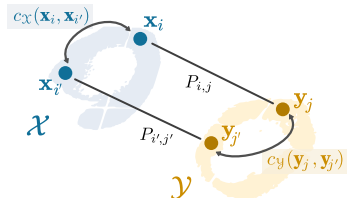
$$\mathcal{FGW}_\alpha^\varepsilon(\mu_t, \nu_t) = \min_{\mathbf{P} \in \mathcal{U}(\mathbf{a}, \mathbf{b})} (1 - \alpha) \mathbf{L}(\mathbf{P}) + \alpha \mathbf{Q}(\mathbf{P}) - \varepsilon \mathbf{E}(\mathbf{P})$$

$$\sum_{i,j} c(\mathbf{x}_i, \mathbf{y}_j) P_{i,j}$$

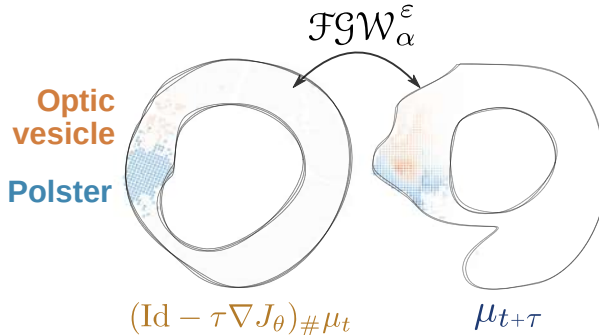
Linear term $\mathbf{L}(\mathbf{P})$
on gene expression

$$\sum_{i,j,i',j'} |c_x(\mathbf{x}_i, \mathbf{x}_{i'}) - c_y(\mathbf{y}_j, \mathbf{y}_{j'})|^2 P_{i,j} P_{i',j'}$$

Quadratic term $\mathbf{Q}(\mathbf{P})$
on spatial coordinates

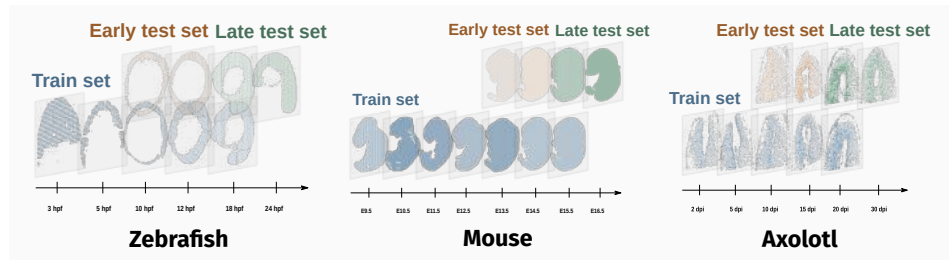


Introducing spatial information with Fused Gromov-Wasserstein



Fused Gromov-Wasserstein leads to improved spatial coherence.

Benchmarking datasets: zebrafish, axolotl, and mouse

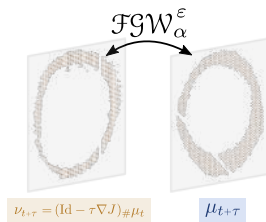


We consider three datasets^{43,44,45}: zebrafish, mouse, and axolotl.

We split the data into a **train set**, **early test set**, and **late test set**.

⁴³Liu et al., *Developmental Cell*, 2022; ⁴⁴Chen et al., *Cell*, 2022; ⁴⁵Wei et al., *Science*, 2022

Evaluation metrics



We evaluate predictions on the test set based on two metrics

$$\mathcal{FGW}_\alpha^\varepsilon(\mu_{t+\tau}, \nu_{t+\tau}) = \min_{\mathbf{P} \in \mathcal{U}(\mathbf{a}, \mathbf{b})} (1 - \alpha) \mathbf{L}(\mathbf{P}) + \alpha \mathbf{Q}(\mathbf{P}) - \varepsilon \mathbf{E}(\mathbf{P})$$

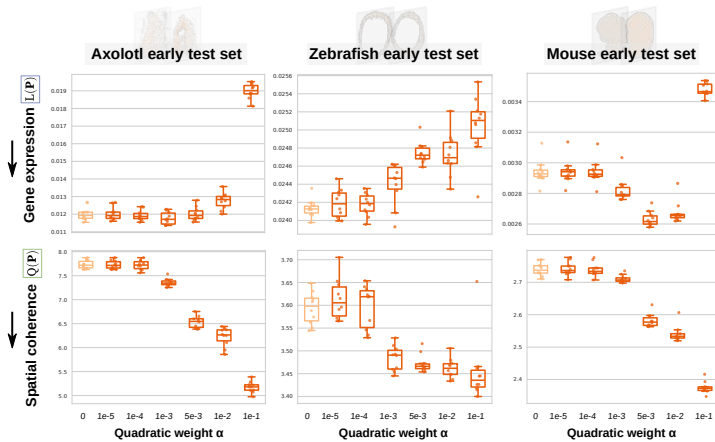
Gene expression **Spatial coherence**

Results on early time points

$$\text{FGW}_{\alpha}^{\varepsilon} = (1 - \alpha) [\mathbf{L}(\mathbf{P}) + \alpha \mathbf{Q}(\mathbf{P})] - \varepsilon \mathbf{E}(\mathbf{P})$$

$(\text{Id} - \tau \nabla J)_\# \mu_t$

$\mu_{t+\tau}$

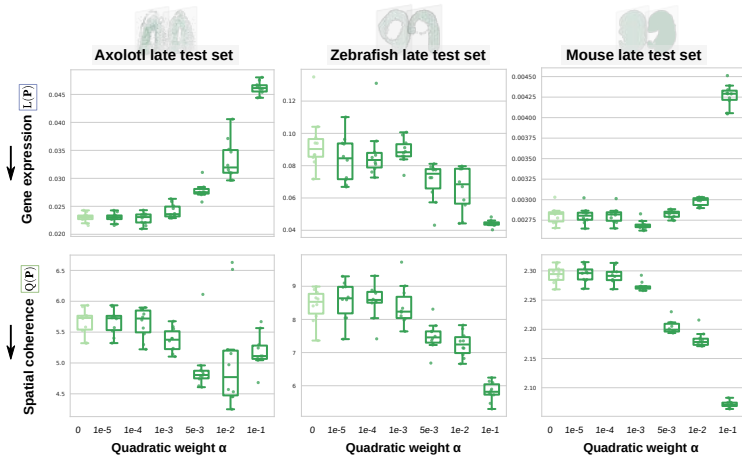


Results on late time points

$$\mathcal{FGW}_\alpha^\varepsilon = (1 - \alpha) \mathbf{L}(\mathbf{P}) + \alpha \mathbf{Q}(\mathbf{P}) - \varepsilon \mathbf{E}(\mathbf{P})$$

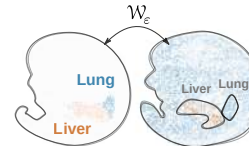
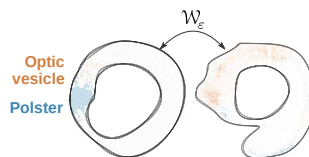
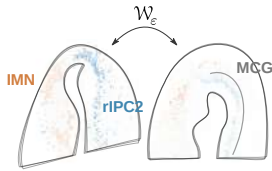
$(\text{Id} - \tau \nabla J) \# \mu_t$

$\mu_{t+\tau}$

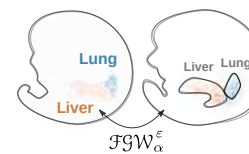
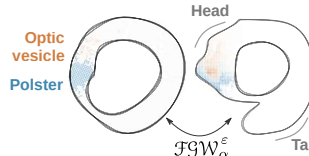
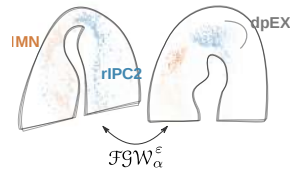


Improved spatial coherence in the matchings

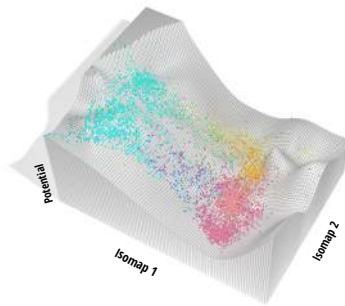
Linear loss



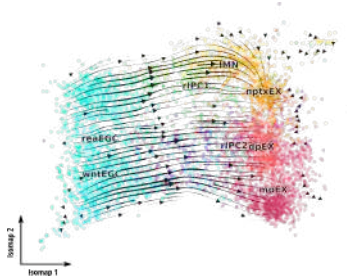
STORIES's loss



Learning a potential of axolotl neuron regeneration

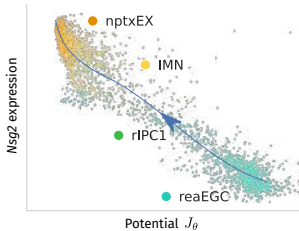
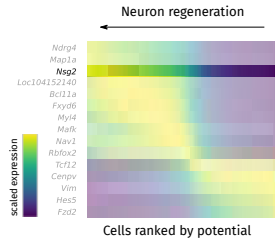


We computed a potential landscape of neuron regeneration in axolots⁴⁶.

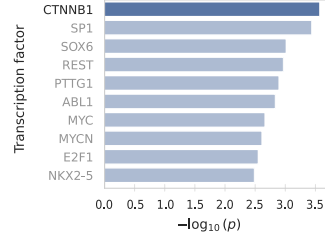


Gradients of this potential confirm a transition from EGCs to mature neurons.

Analyzing the dynamics of neuron regeneration

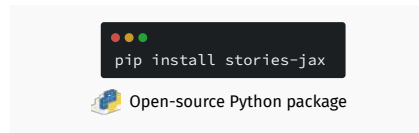
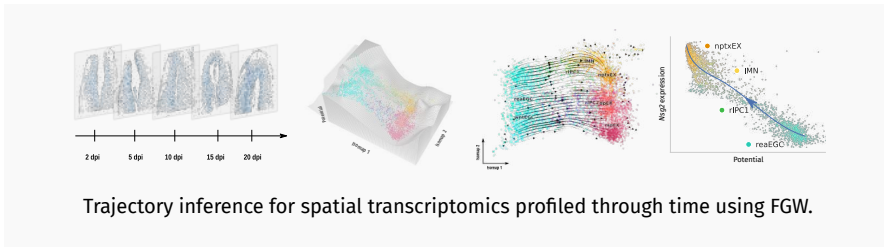


We identify potential driver genes by regressing their expression based on the potential.



Transcription Factors targeting these genes represent candidate regulators.

Conclusion



Introduction
oooooooooooo

OT as a cell-cell distance
oooooooooooo

Wasserstein Singular Vectors
oooooooooooo

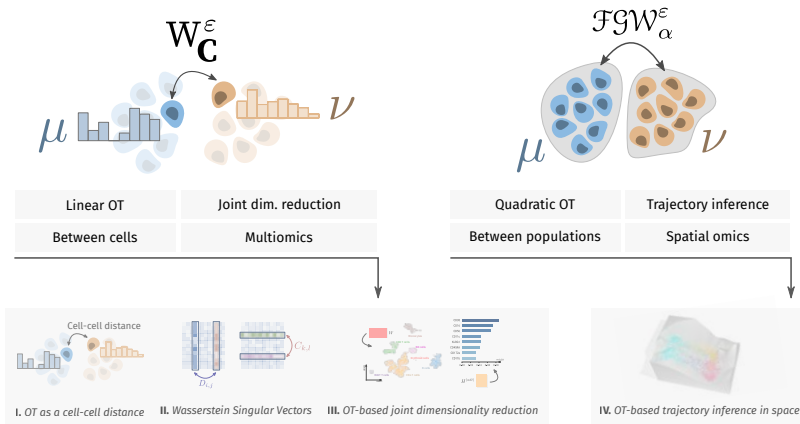
OT-based joint dimensionality reduction
oooooooooooo

OT-based trajectory inference
oooooooooooooooooooo

Conclusion
●oooooo

Conclusion

Contributions



^IHuizing et al., *Bioinformatics*, 2022; ^{II}Huizing et al., *ICML*, 2022; ^{III}Huizing et al., *Nat. Comm.*, 2023; ^{IV}Huizing et al., *bioRxiv*, 2024

Perspectives: OT computation at the scale of single-cell atlases



The increased availability of large multimodal atlases motivates fast approximations of OT.



Graph diffusion-based⁴⁷



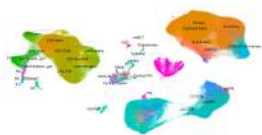
Tree-based⁴⁸



Neural network-based^{49,50}

⁴⁷Tong et al., ICASSP, 2022; ⁴⁸Düsterwald et al., ICML GRaM Workshop, 2024; ⁴⁹Courty et al., ICLR, 2018; ⁵⁰Haviv et al., ICML, 2024

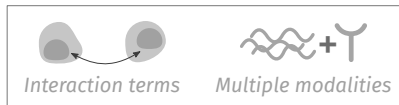
Perspectives: Methodological improvements for further biological insights



Finding rare cell types and complex cellular dynamics motivates further methodological improvements.



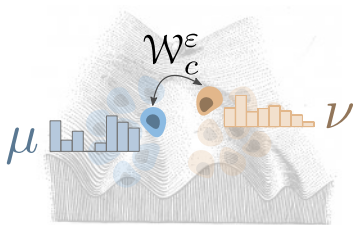
Nonlinear joint dimensionality reduction⁵¹.



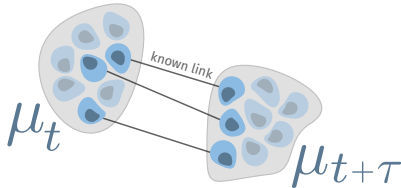
More general class of differentiation potentials^{52,53}.

⁵¹Schmitz et al., SIAM Journal on Imaging Sciences, 2018; ⁵²Weinreb et al., PNAS, 2018; ⁵³Terpin et al., arXiv, 2024

Perspectives: Unified OT framework for multimodal omics data



Hierarchical OT framework
for population dynamics⁵⁴.



Ground metric learning from partial
pairings in time-course data^{55,56}.

⁵⁴Yurochkin et al., NeurIPS, 2019; ⁵⁵Dupuy and Galichon, *Journal of Political Economy*, 2014; ⁵⁶Chen et al., *Nature*, 2022

Acknowledgements

Jury members

Ahmed Mahfouz

Franck Picard

Andrea Rau

Laurence Calzone

Lorette Noiret

Laura Cantini

Gabriel Peyré

ML4IG lab • Institut Pasteur, CSD • ENS, and more!

